JOURNAL OF SPACECRAFT AND ROCKETS
Vol. 46, No. 6, November–December 2009

Engineering Notes

Linear Feedback Guidance for Low-Thrust Many-Revolution Earth-Orbit Transfers

Yang Gao*
Chinese Academy of Sciences, 100190 Beijing, People's Republic of China

DOI: 10.2514/1.43395

Introduction

TO GUIDE a low-thrust spacecraft to a target orbit, the most commonly used strategy is to frequently uplink control commands to correct orbital deviations. However, this guidance scheme requires a large amount of offline optimal control computations and data communications between the ground and the spacecraft, especially for low-thrust many-revolution Earth-orbit transfer missions (which may last several months). For the purpose of reducing ground operational loads, autonomous guidance has to be placed onboard. Kluever developed an inverse dynamics approach [1] and an empirical control law [2] to track reference trajectories, based on the concept of predictive control. These two methods require onboard iterative algorithms to find appropriate control-related parameters. In engineering practice, the implementation of the predictive control guidance usually depends on accurate calibration of thrust magnitude and direction as well as predictive horizon. Another strategy of low-thrust autonomous guidance is based on Lyapunov control laws [3–6] (which, however, usually do not provide optimal solutions). The question of how to select feedback gains of the Lyapunov control laws to achieve optimal or near-optimal performance is still unresolved.

In this study, a new linear feedback guidance scheme is proposed for low-thrust Earth-orbit transfers involving large numbers of orbital revolutions. The key concept of this guidance scheme is that the spacecraft tracks the nominal trajectory, which is expressed by mean orbital elements without involving short periodic osculating motion. First, optimal trajectory and control are obtained via a direct optimization method with the consideration of both J_2 perturbations and shadowing conditions. Along the optimal trajectory and control, a set of linearized equations of spacecraft motion expressed by mean orbital elements is then developed. At last, the trajectory tracking problem is formulated as a standard time-varying linear control problem, and linear control theory can be readily used for designing the guidance control law. An example transfer from a geostationary transfer orbit (GTO) to a geostationary orbit (GEO) was simulated to verify the guidance performance.

Generation of Nominal Trajectory and Control Using Direct Optimization

A set of nonsingular equinoctial elements $\boldsymbol{x} = [p \quad f \quad g \quad h \quad k \quad L]$ is employed to govern the spacecraft dynamics [7,8]. The equinoctial elements in terms of the classical orbital elements $[a \quad e \quad i \quad \Omega \quad \omega \quad \theta]$ (semimajor axis, eccentricity, inclination, longitude of ascending node, argument of perigee, and true anomaly) are given by $p = a(1-e^2)$, $f = e\cos(\omega+\Omega)$, $g = e\sin(\omega+\Omega)$, $h = \tan(i/2)\cos\Omega$, $k = \tan(i/2)\sin\Omega$, and $L = \Omega + \omega + \theta$. The equation of motion for the spacecraft can be written in the following matrix form:

$$\dot{\boldsymbol{x}} = \boldsymbol{M}[(T/m)\boldsymbol{\alpha} + \boldsymbol{\beta}] + \boldsymbol{D} \tag{1}$$

where $\boldsymbol{M}$ is a 6×3 matrix and $\boldsymbol{D}$ is a 6×1 vector (see [7,8]), T is the thrust magnitude, m is the spacecraft mass, and $\boldsymbol{\alpha} = [\alpha_1 \quad \alpha_2 \quad \alpha_3]^T$ and $\boldsymbol{\beta} = [\beta_1 \quad \beta_2 \quad \beta_3]^T$ are the unit vector of the thrust direction and the vector of perturbation acceleration, respectively, in the local-vertical local-horizontal (LVLH) frame. Note that the thrust direction $\boldsymbol{\alpha}$ can also be expressed by the pitch δ and yaw ϕ angles in the LVLH frame. The instantaneous mass flow rate is computed by $\dot{m} = -T/(g_e I_{sp})$, where g_e is the gravitational acceleration at sea level and I_{sp} is the specific impulse. Assuming that the low-thrust acceleration is much smaller than the gravitational acceleration, the time rate of the equinoctial element L can be approximated as

$$\frac{\mathrm{d}L}{\mathrm{d}t} \approx \sqrt{\mu p}\left(\frac{1 + f\cos L + g\sin L}{p}\right)^2 \tag{2}$$

The first-order time rates of the mean equinoctial elements (defined as $\bar{\boldsymbol{x}} = [\bar{p} \quad \bar{f} \quad \bar{g} \quad \bar{h} \quad \bar{k}]$) can be computed as (based on the orbital averaging method)

$$\dot{\bar{\boldsymbol{x}}} \approx \frac{1}{P}\int_0^{2\pi} \dot{\boldsymbol{x}} \frac{\mathrm{d}t}{\mathrm{d}L}\,\mathrm{d}L \tag{3}$$

where P is the orbital period. Using Eqs. (1) and (2), a further expression of Eq. (3) is

$$\dot{\bar{\boldsymbol{x}}} = \frac{1}{2\pi}(1 - \bar{f}^2 - \bar{g}^2)^{3/2}\left[\int_{L_1}^{L_2} \frac{\boldsymbol{f}^{(LT)}(\bar{\boldsymbol{x}}, L, \boldsymbol{\alpha})}{(1 + \bar{f}\cos L + \bar{g}\sin L)^2}\,\mathrm{d}L + \int_0^{2\pi} \frac{\boldsymbol{f}^{(PB)}(\bar{\boldsymbol{x}}, L, \boldsymbol{\beta})}{(1 + \bar{f}\cos L + \bar{g}\sin L)^2}\,\mathrm{d}L\right] \tag{4}$$

where $\boldsymbol{f}^{(LT)}(\bar{\boldsymbol{x}}, L, \boldsymbol{\alpha}) = (T/m)\bar{\boldsymbol{M}}\boldsymbol{\alpha}$ is caused by low thrust and $\boldsymbol{f}^{(PB)}(\bar{\boldsymbol{x}}, L, \boldsymbol{\beta}) = \bar{\boldsymbol{M}}\boldsymbol{\beta}$ by perturbations. The matrix $\bar{\boldsymbol{M}}$ is in 5×3 dimension (removing the sixth row of $\boldsymbol{M}$), and its elements are the functions of $\bar{\boldsymbol{x}} = [\bar{p} \quad \bar{f} \quad \bar{g} \quad \bar{h} \quad \bar{k}]$ and L. The integral limits L_1 and L_2 in Eq. (4) denote shadow exit and entrance angles, respectively. If the spacecraft is in the shadow, the thrust is off. Likewise, the averaged mass flow rate is computed as

$$\dot{\bar{m}} = \frac{1}{2\pi}(1 - \bar{f}^2 - \bar{g}^2)^{3/2}\int_{L_1}^{L_2} \frac{\dot{m}}{(1 + \bar{f}\cos L + \bar{g}\sin L)^2}\,\mathrm{d}L \tag{5}$$

The definite integrals in Eqs. (4) and (5) can be approximately computed by the Gauss–Legendre quadrature. Because of the slow evolution of the mean equinoctial elements $\bar{\boldsymbol{x}} = [\bar{p} \quad \bar{f} \quad \bar{g} \quad \bar{h} \quad \bar{k}]$, Eqs. (4) and (5) can be integrated with large time steps, such as one or two days, which significantly alleviate the computational burden compared with the precisely propagating osculating orbital elements. More detailed information of the orbital averaging method can be found in [9,10].

According to optimal control theory (or the calculus of variations) [11], with a cost function in terms of the Mayer form $J = \varphi(\bar{\boldsymbol{x}}(t_f), \bar{m}(t_f), t_f)$ (where t_f is the terminal time), the Hamiltonian system is formulated as $\bar{H} = \bar{\boldsymbol{\lambda}}^T\dot{\bar{\boldsymbol{x}}} + \bar{\lambda}_m\dot{\bar{m}}$ [using the averaged dynamics (4) and (5)], where $\bar{\boldsymbol{\lambda}} = [\bar{\lambda}_p \quad \bar{\lambda}_f \quad \bar{\lambda}_g \quad \bar{\lambda}_h \quad \bar{\lambda}_k]^T$ is the costate vector

Received 22 January 2009; revision received 07 August 2009; accepted for publication 08 August 2009.

*Associate Research Fellow, Academy of Opto-Electronics, Department of Space System Engineering. Post Office Box 8701; GaoY@aoe.ac.cn.

associated with the corresponding mean equinoctial elements $\bar{\boldsymbol{x}} = [\bar{p} \quad \bar{f} \quad \bar{g} \quad \bar{h} \quad \bar{k}]$ and $\bar{\lambda}_m$ is the costate variable associated with the spacecraft mass $\bar{m}$. The optimal thrust direction unit vector $\boldsymbol{\alpha}^*$ is obtained by setting $\partial \bar{H}/\partial \boldsymbol{\alpha} = 0$ with the constraint $\boldsymbol{\alpha}^T\boldsymbol{\alpha} = 1$:

$$\boldsymbol{\alpha}^* = -\frac{\bar{\boldsymbol{M}}^T\bar{\boldsymbol{\lambda}}}{\|\bar{\boldsymbol{M}}^T\bar{\boldsymbol{\lambda}}\|} \tag{6}$$

In this study, the control law in Eq. (6) is applied in each orbital revolution and $\bar{\boldsymbol{\lambda}}$ is considered a parameter vector that governs the control law. For convenience, the term *controller parameter vector* is used to denote $\bar{\boldsymbol{\lambda}}$.

The time history of the controller parameter vector $\bar{\boldsymbol{\lambda}}(t)$ is interpolated through a number of nodal values along the time history instead of being governed by the differential costate equation $\dot{\bar{\boldsymbol{\lambda}}} = -\partial \bar{H}/\partial \bar{\boldsymbol{x}}$. The averaged dynamics in Eqs. (4) and (5) are numerically integrated from the initial time to the terminal time. The optimal control problem is converted to the parameter optimization problem that is solved by nonlinear programming: sequential quadratic programming (SQP) [12]. In the problem of the SQP, the performance index can be set as minimum fuel, minimum time, and so on; the constraints are set as the target orbital elements at the terminal time of the transfer; and the optimization variables are the nodal values for interpolating $\bar{\boldsymbol{\lambda}}(t)$ and the transfer time (or the terminal time t_f). This direct optimization method is categorized as a direct shooting method that, in general, results in better convergence robustness than the indirect shooting method [13]. However, the converged solution obtained in this study will not be verified a posteriori to satisfy all the first-order necessary optimality conditions [11] that are derived from the optimal control theory.

Linearization Along Nominal Trajectory and Control

The linearized equation of motion about the nominal trajectory and control can be derived in the following form:

$$\delta\dot{\bar{\boldsymbol{x}}}(t) = \boldsymbol{A}(t)\delta\bar{\boldsymbol{x}}(t) + \boldsymbol{B}(t)\delta\bar{\boldsymbol{\lambda}}(t) \tag{7}$$

where

$$\boldsymbol{A}(t) = \left.\frac{\partial \boldsymbol{F}(\bar{\boldsymbol{x}}, \bar{\boldsymbol{\lambda}})}{\partial \bar{\boldsymbol{x}}}\right|_{\bar{\boldsymbol{x}}^*(t), \bar{\boldsymbol{\lambda}}^*(t)}, \qquad \boldsymbol{B}(t) = \left.\frac{\partial \boldsymbol{F}(\bar{\boldsymbol{x}}, \bar{\boldsymbol{\lambda}})}{\partial \bar{\boldsymbol{\lambda}}}\right|_{\bar{\boldsymbol{x}}^*(t), \bar{\boldsymbol{\lambda}}^*(t)} \tag{8}$$

In Eq. (7), $\delta\bar{\boldsymbol{x}}(t) = \bar{\boldsymbol{x}}(t) - \bar{\boldsymbol{x}}^*(t)$ and $\delta\bar{\boldsymbol{\lambda}}(t) = \bar{\boldsymbol{\lambda}}(t) - \bar{\boldsymbol{\lambda}}^*(t)$. The state and control of the nominal transfer trajectory denoted by $\bar{\boldsymbol{x}}^*(t)$ and $\bar{\boldsymbol{\lambda}}^*(t)$ are obtained through the optimization method presented in the preceding section. Note that Eq. (5) is not involved in the linearization. The expression of $\boldsymbol{F}(\bar{\boldsymbol{x}}, \bar{\boldsymbol{\lambda}})$ in Eq. (8) is shown as the right-hand side of Eq. (4):

$$\boldsymbol{F}(\bar{\boldsymbol{x}}, \bar{\boldsymbol{\lambda}}) = \xi_1(\bar{\boldsymbol{x}})\left[\int_{L_1}^{L_2} \boldsymbol{\xi}^{(LT)}(\bar{\boldsymbol{x}}, \bar{\boldsymbol{\lambda}}, L)\,\mathrm{d}L + \int_0^{2\pi} \boldsymbol{\xi}^{(PB)}(\bar{\boldsymbol{x}}, L)\,\mathrm{d}L\right] \tag{9}$$

where

$$\xi_1(\bar{\boldsymbol{x}}) = \frac{1}{2\pi}(1 - \bar{f}^2 - \bar{g}^2)^{3/2} \tag{10}$$

$$\boldsymbol{\xi}^{(LT)}(\bar{\boldsymbol{x}}, \bar{\boldsymbol{\lambda}}, L) = \phi(\bar{\boldsymbol{x}}, L)\boldsymbol{f}^{(LT)}(\bar{\boldsymbol{x}}, \bar{\boldsymbol{\lambda}}, L) \tag{11}$$

$$\boldsymbol{\xi}^{(PB)}(\bar{\boldsymbol{x}}, L) = \phi(\bar{\boldsymbol{x}}, L)\boldsymbol{f}^{(PB)}(\bar{\boldsymbol{x}}, L) \tag{12}$$

$$\phi(\bar{\boldsymbol{x}}, L) = \frac{1}{(1 + \bar{f}\cos L + \bar{g}\sin L)^2} \tag{13}$$

An approximation is made based on the assumption that the small deviation $\delta\bar{\boldsymbol{x}}(t)$ does not affect the shadow exit and entrance angles (L_1 and L_2) along the nominal trajectory, which implies that the term $\frac{\partial \boldsymbol{F}}{\partial L_i}\frac{\partial L_i}{\partial \bar{\boldsymbol{x}}}$ ($i = 1, 2$) is not included in deriving $\boldsymbol{A}(t)$ in Eq. (7). If there is no shadow (i.e., $L_1 = 0$ and $L_2 = 2\pi$), this approximation is not necessary.

Partial Derivatives of $\boldsymbol{F}(\bar{\boldsymbol{x}}, \bar{\boldsymbol{\lambda}})$ with Respect to the State Vector $\bar{\boldsymbol{x}}$

According to the definition of the partial derivatives of scalar and vector functions with multiple variables, the partial derivative of $\boldsymbol{F}(\bar{\boldsymbol{x}}, \bar{\boldsymbol{\lambda}})$ with respect to $\bar{\boldsymbol{x}}$ is

$$\begin{aligned}\boldsymbol{A}(t) = \frac{\partial \boldsymbol{F}(\bar{\boldsymbol{x}}, \bar{\boldsymbol{\lambda}})}{\partial \bar{\boldsymbol{x}}} &= \xi_1(\bar{\boldsymbol{x}})\left[\int_{L_1}^{L_2} \frac{\partial \boldsymbol{\xi}^{(LT)}(\bar{\boldsymbol{x}}, \bar{\boldsymbol{\lambda}}, L)}{\partial \bar{\boldsymbol{x}}}\,\mathrm{d}L\right. \\ &\left.+ \int_0^{2\pi} \frac{\partial \boldsymbol{\xi}^{(PB)}(\bar{\boldsymbol{x}}, L)}{\partial \bar{\boldsymbol{x}}}\,\mathrm{d}L\right] + \left[\int_{L_1}^{L_2} \boldsymbol{\xi}^{(LT)}(\bar{\boldsymbol{x}}, \bar{\boldsymbol{\lambda}}, L)\,\mathrm{d}L\right. \\ &\left.+ \int_0^{2\pi} \boldsymbol{\xi}^{(PB)}(\bar{\boldsymbol{x}}, L)\,\mathrm{d}L\right]\left[\frac{\partial \xi_1(\bar{\boldsymbol{x}})}{\partial \bar{\boldsymbol{x}}}\right]^T\end{aligned} \tag{14}$$

The partial derivative of $\xi_1(\bar{\boldsymbol{x}})$ with respect to $\bar{\boldsymbol{x}}$ can be readily derived, but the trivial derivation is not presented herein. The partial derivatives of $\boldsymbol{\xi}^{(LT)}(\bar{\boldsymbol{x}}, \bar{\boldsymbol{\lambda}}, L)$ and $\boldsymbol{\xi}^{(PB)}(\bar{\boldsymbol{x}}, L)$ with respect to $\bar{\boldsymbol{x}}$ are

$$\begin{aligned}\frac{\partial \boldsymbol{\xi}^{(LT)}(\bar{\boldsymbol{x}}, \bar{\boldsymbol{\lambda}}, L)}{\partial \bar{\boldsymbol{x}}} &= \phi(\bar{\boldsymbol{x}}, L)\frac{\partial \boldsymbol{f}^{(LT)}(\bar{\boldsymbol{x}}, \bar{\boldsymbol{\lambda}}, L)}{\partial \bar{\boldsymbol{x}}} \\ &+ \boldsymbol{f}^{(LT)}(\bar{\boldsymbol{x}}, \bar{\boldsymbol{\lambda}}, L)\left[\frac{\partial \phi(\bar{\boldsymbol{x}}, L)}{\partial \bar{\boldsymbol{x}}}\right]^T\end{aligned} \tag{15}$$

$$\frac{\partial \boldsymbol{\xi}^{(PB)}(\bar{\boldsymbol{x}}, L)}{\partial \bar{\boldsymbol{x}}} = \phi(\bar{\boldsymbol{x}}, L)\frac{\partial \boldsymbol{f}^{(PB)}(\bar{\boldsymbol{x}}, L)}{\partial \bar{\boldsymbol{x}}} + \boldsymbol{f}^{(PB)}(\bar{\boldsymbol{x}}, L)\left[\frac{\partial \phi(\bar{\boldsymbol{x}}, L)}{\partial \bar{\boldsymbol{x}}}\right]^T \tag{16}$$

Likewise, deriving the partial derivatives of $\phi(\bar{\boldsymbol{x}}, L)$ with respect to $\bar{\boldsymbol{x}}$ is straightforward. The remaining problem is to compute the partial derivatives of $\boldsymbol{f}^{(LT)}(\bar{\boldsymbol{x}}, \bar{\boldsymbol{\lambda}}, L)$ and $\boldsymbol{f}^{(PB)}(\bar{\boldsymbol{x}}, L)$ with respect to $\bar{\boldsymbol{x}}$. Based on the control law in Eq. (6), the following expression is obtained:

$$\boldsymbol{f}^{(LT)}(\bar{\boldsymbol{x}}, \bar{\boldsymbol{\lambda}}, L) = \frac{T}{m}\bar{\boldsymbol{M}}\boldsymbol{\alpha}^* = -\frac{T}{m}\bar{\boldsymbol{M}}\frac{\bar{\boldsymbol{M}}^T\bar{\boldsymbol{\lambda}}}{\|\bar{\boldsymbol{M}}^T\bar{\boldsymbol{\lambda}}\|} \tag{17}$$

With the elements in the matrices and vectors, $\boldsymbol{f}^{(LT)}(\bar{\boldsymbol{x}}, \bar{\boldsymbol{\lambda}}, L)$ can be written as

$$\begin{aligned}\boldsymbol{f}^{(LT)}(\bar{\boldsymbol{x}}, \bar{\boldsymbol{\lambda}}, L) &= -\frac{T}{m}\begin{bmatrix} f_1^{(LT)}(\bar{\boldsymbol{x}}, \bar{\boldsymbol{\lambda}}, L) \\ f_2^{(LT)}(\bar{\boldsymbol{x}}, \bar{\boldsymbol{\lambda}}, L) \\ \cdots \\ f_5^{(LT)}(\bar{\boldsymbol{x}}, \bar{\boldsymbol{\lambda}}, L) \end{bmatrix} \\ &= -\frac{T}{m}\begin{bmatrix} \overline{M}_{11}\alpha_1 + \overline{M}_{12}\alpha_2 + \overline{M}_{13}\alpha_3 \\ \overline{M}_{21}\alpha_1 + \overline{M}_{22}\alpha_2 + \overline{M}_{23}\alpha_3 \\ \cdots \\ \overline{M}_{51}\alpha_1 + \overline{M}_{52}\alpha_2 + \overline{M}_{53}\alpha_3 \end{bmatrix}\alpha_T^{-1/2}\end{aligned} \tag{18}$$

where

$$\alpha_j = \sum_{s=1}^{5} \bar{M}_{sj}\bar{\lambda}_s, \qquad j = 1, 2, 3 \tag{19}$$

$$\alpha_T = \alpha_1^2 + \alpha_2^2 + \alpha_3^2 \tag{20}$$

The partial derivative of $f_i^{(LT)}(\bar{\boldsymbol{x}}, \bar{\boldsymbol{\lambda}}, L)$ ($i = 1, 2, \ldots, 5$) with respect to $\bar{x}_n$ ($n = 1, 2, \ldots, 5$) is derived as

$$\frac{\partial f_i^{(LT)}}{\partial \bar{x}_n} = \alpha_T^{-1/2}\left[\sum_{j=1}^{3}\left(\frac{\partial \bar{M}_{ij}}{\partial \bar{x}_n}\alpha_j\right) + \sum_{j=1}^{3}\left(\bar{M}_{ij}\frac{\partial \alpha_j}{\partial \bar{x}_n}\right)\right] - \alpha_T^{-3/2}\left[\sum_{j=1}^{3}\left(\alpha_j\frac{\partial \alpha_j}{\partial \bar{x}_n}\right)\right]\left[\sum_{j=1}^{3}(\bar{M}_{ij}\alpha_j)\right] \tag{21}$$

where

$$\frac{\partial \alpha_j}{\partial \bar{x}_n} = \sum_{s=1}^{5}\frac{\partial \bar{M}_{sj}}{\partial \bar{x}_n}\bar{\lambda}_s, \qquad i = 1, 2, \ldots, 5; \qquad j = 1, 2, 3; \qquad n = 1, 2, \ldots, 5 \tag{22}$$

It is shown by Eqs. (21) and (22) that obtaining $\partial \boldsymbol{f}^{(LT)}/\partial \bar{\boldsymbol{x}}$ finally requires the partial derivatives of each element in the matrix $\bar{\boldsymbol{M}}$ with respect to each equinoctial element $\bar{x}_n$ ($n = 1, 2, \ldots, 5$) (see [8]).

The perturbation function $\boldsymbol{f}^{(PB)}(\bar{\boldsymbol{x}}, L)$ can be written as

$$\boldsymbol{f}^{(PB)}(\bar{\boldsymbol{x}}, L) = \begin{bmatrix} f_1^{(PB)}(\bar{\boldsymbol{x}}, L) \\ f_2^{(PB)}(\bar{\boldsymbol{x}}, L) \\ \cdots \\ f_5^{(PB)}(\bar{\boldsymbol{x}}, L) \end{bmatrix} = \begin{bmatrix} \overline{M}_{11}\beta_1 + \overline{M}_{12}\beta_2 + \overline{M}_{13}\beta_3 \\ \overline{M}_{21}\beta_1 + \overline{M}_{22}\beta_2 + \overline{M}_{23}\beta_3 \\ \cdots \\ \overline{M}_{51}\beta_1 + \overline{M}_{52}\beta_2 + \overline{M}_{53}\beta_3 \end{bmatrix} \tag{23}$$

To obtain $\partial \boldsymbol{f}^{(PB)}/\partial \bar{\boldsymbol{x}}$, it is necessary to compute the partial derivatives of $f_i^{(PB)}$ ($i = 1, 2, \ldots, 5$) with respect to each equinoctial element $\bar{x}_n$ ($n = 1, 2, \ldots, 5$):

$$\frac{\partial f_i^{(PB)}}{\partial \bar{x}_n} = \sum_{j=1}^{3}\left(\frac{\partial \bar{M}_{ij}}{\partial \bar{x}_n}\beta_j\right) + \sum_{j=1}^{3}\left(\bar{M}_{ij}\frac{\partial \beta_j}{\partial \bar{x}_n}\right), \qquad n = 1, 2, \ldots, 5 \tag{24}$$

If J_2 perturbations are included, the three components of the perturbing acceleration expressed by the equinoctial elements in the LVLH frame can be expressed as

$$\boldsymbol{\beta} = \begin{bmatrix} \beta_1 \\ \beta_2 \\ \beta_3 \end{bmatrix} = \begin{Bmatrix} -\frac{3\mu J_2 R_e^2}{2r^4}\left[1 - \frac{12(\bar{h}\sin L - \bar{k}\cos L)^2}{(1+\bar{h}^2+\bar{k}^2)^2}\right] \\ -\frac{12\mu J_2 R_e^2}{r^4}\frac{(\bar{h}\sin L - \bar{k}\cos L)(\bar{h}\cos L + \bar{k}\sin L)}{(1+\bar{h}^2+\bar{k}^2)^2} \\ -\frac{6\mu J_2 R_e^2}{r^4}\frac{(1-\bar{h}^2-\bar{k}^2)(\bar{h}\sin L - \bar{k}\cos L)}{(1+\bar{h}^2+\bar{k}^2)^2} \end{Bmatrix} \tag{25}$$

where μ is the gravitational parameter of the Earth, R_e is the Earth radius, and r is the orbital radius computed by the equinoctial elements $r = \bar{p}/(1 + \bar{f}\cos L + \bar{g}\sin L)$. Likewise, it is straightforward to compute the derivatives of each element in the vector $\boldsymbol{\beta}$ with respect to $\bar{\boldsymbol{x}}$.

Partial Derivatives of $F(\bar{x}, \bar{\lambda})$ with Respect to the Controller Parameter Vector $\bar{\lambda}$

To obtain the matrix $\boldsymbol{B}(t)$ in Eq. (7), the partial derivative of $\boldsymbol{F}(\bar{\boldsymbol{x}}, \bar{\boldsymbol{\lambda}})$ with respect to $\bar{\boldsymbol{\lambda}}$ is derived as

$$\boldsymbol{B}(t) = \frac{\partial \boldsymbol{F}(\bar{\boldsymbol{x}}, \bar{\boldsymbol{\lambda}})}{\partial \bar{\boldsymbol{\lambda}}} = \xi_1(\bar{\boldsymbol{x}})\int_{L_1}^{L_2}\phi(\bar{\boldsymbol{x}}, L)\frac{\partial \boldsymbol{f}^{(LT)}(\bar{\boldsymbol{x}}, \bar{\boldsymbol{\lambda}}, L)}{\partial \bar{\boldsymbol{\lambda}}}\,\mathrm{d}L \tag{26}$$

Note that there is no derivative of the perturbation function $\boldsymbol{f}^{(PB)}(\bar{\boldsymbol{x}}, L)$ with respect to $\bar{\boldsymbol{\lambda}}$, which can be shown by Eqs. (9) and (12). According to Eq. (26), it is necessary to derive the partial derivatives of $f_i^{(LT)}(\bar{\boldsymbol{x}}, \bar{\boldsymbol{\lambda}}, L)$ ($i = 1, 2, \ldots, 5$) with respect to $\bar{\lambda}_n$ ($n = 1, 2, \ldots, 5$):

$$\frac{\partial f_i^{(LT)}}{\partial \bar{\lambda}_n} = \alpha_T^{-1/2}\left[\sum_{j=1}^{3}\left(\bar{M}_{ij}\frac{\partial \alpha_j}{\partial \bar{\lambda}_n}\right)\right] - \alpha_T^{-3/2}\left[\sum_{j=1}^{3}\left(\alpha_j\frac{\partial \alpha_j}{\partial \bar{\lambda}_n}\right)\right]\left[\sum_{j=1}^{3}(\bar{M}_{ij}\alpha_j)\right] \tag{27}$$

where

$$\frac{\partial \alpha_j}{\partial \bar{\lambda}_n} = \bar{M}_{nj}, \qquad j = 1, 2, 3; \qquad n = 1, 2, \ldots, 5 \tag{28}$$

The definite integrals for obtaining $\boldsymbol{A}(t)$ and $\boldsymbol{B}(t)$ in Eqs. (14) and (26) are approximately computed using the Gauss–Legendre quadrature.

Feedback Guidance Design Using Linear Quadratic Regulator

In the previous section, a standard time-varying linear control system is generalized in Eq. (7). The feedback control law can be formulated as $\delta\bar{\boldsymbol{\lambda}} = -\boldsymbol{K}\delta\bar{\boldsymbol{x}}$ for trajectory tracking. A systematic method to compute the feedback gain $\boldsymbol{K}$ is the finite-horizon linear quadratic regulator (LQR) approach in which backward integration of the differential Riccati equation is required [14]. Additionally, it is worth noting that Eq. (7) represents a slowly time-varying dynamical system because of the use of the orbital averaging method. Furthermore, the time horizon of the entire transfer can be divided into a number of small time intervals (termed subintervals herein), which could be an integration time step such as one or two days for accurately propagating mean orbital elements. Over each subinterval, the linear control system can be approximately considered time invariant. Therefore, the linear time-invariant control system over the corresponding subinterval can be stabilized independently, which yields an adaptive control strategy along the time history of the transfer. Note that the number of those subintervals will not be quite large owing to the use of the orbital averaging method.

In this note, the steady-state LQR is devised for each finite-horizon time-invariant control system [14]. At the initial time instant t_i of each subinterval, the cost function to be minimized is set as

$$J_{\mathrm{LQR}} = \int_{t_i}^{\infty}(\delta\bar{\boldsymbol{x}}^T\boldsymbol{Q}\delta\bar{\boldsymbol{x}} + \delta\bar{\boldsymbol{\lambda}}^T\boldsymbol{R}\delta\bar{\boldsymbol{\lambda}})\,\mathrm{d}t \tag{29}$$

where $\boldsymbol{Q}$ and $\boldsymbol{R}$ are positive definite diagonal matrices defined a priori. The feedback gain $\boldsymbol{K}$ is computed by $\boldsymbol{K} = \boldsymbol{R}^{-1}\boldsymbol{B}^T\boldsymbol{S}$, where $\boldsymbol{S}$ is obtained by solving the algebraic Riccati equation (ARE):

$$\boldsymbol{A}^T\boldsymbol{S} + \boldsymbol{S}\boldsymbol{A} - \boldsymbol{S}\boldsymbol{B}\boldsymbol{R}^{-1}\boldsymbol{S} + \boldsymbol{Q} = 0 \tag{30}$$

The most fundamental criterion of selecting $\boldsymbol{K}$, relevant to selecting $\boldsymbol{Q}$ and $\boldsymbol{R}$, is to ensure that all the eigenvalues of $\boldsymbol{A} - \boldsymbol{B}\boldsymbol{K}$ for the closed-loop control system $\delta\dot{\bar{\boldsymbol{x}}} = (\boldsymbol{A} - \boldsymbol{B}\boldsymbol{K})\delta\bar{\boldsymbol{x}}$ have negative real parts. The time-varying matrices $\boldsymbol{S}(t)$ and $\boldsymbol{K}(t)$ are obtained by solving a number of AREs along the nominal trajectory and control. For example, if there are 100 integration steps for trajectory propagation, it is necessary to solve 100 AREs at each integration step to obtain 100 nodes for representing $\boldsymbol{S}(t)$ and $\boldsymbol{K}(t)$. However, all these computations can be done offline, and there are many existing programs for solving AREs, such as the LQR function in MATLAB®. The suitability of the proposed control scheme in which a series of steady-state LQRs are implemented will be verified by the subsequent numerical simulations.

Preliminary Numerical Simulations

In this section, the linear feedback control is employed to guide the spacecraft from a GTO ($\bar{a} = 3.82R_e$, $\bar{e} = 0.731$, $\bar{i} = 27$ deg, $\bar{\Omega} = 99$ deg, and $\bar{\omega} = 0$) to a GEO ($\bar{a} = 6.6107R_e$, $\bar{e} = 0$, $\bar{i} = 0$, or $\bar{p} = 6.6107R_e$ and $\bar{f} = \bar{g} = \bar{h} = \bar{k} = 0$) (cited from [15,16]). The nominal thrust magnitude T is 200.853 mN, and the specific impulse I_{sp} is 3300 s. The initial spacecraft mass is 450 kg. The Earth's

Table 1 Uncertainty intervals

Errors in the initial orbit elements	Unknown misalignment in thrust direction angles	Unknown bias in thrust magnitude
$\delta\bar{a}(t_0)$: $[-0.03R_e \quad 0.03R_e]$	Pitch (δ): $[-2 \quad 2]$ deg	$[-10\% \quad 10\%]$ of the nominal thrust magnitude
$\delta\bar{e}(t_0)$: $[-0.04 \quad 0.04]$	Yaw (ϕ): $[-2 \quad 2]$ deg	——
$\delta\bar{i}(t_0)$: $[-1 \quad 1]$ deg	——	——
$\delta\bar{\Omega}(t_0)$: $[-2 \quad 2]$ deg	——	——
$\delta\bar{\omega}(t_0)$: $[-5 \quad +5]$ deg	——	——

shadow and J_2 perturbations are included. The initial date of the transfer is set to 01 January 2008, and the sun's position for computing the Earth's shadow is obtained by the Jet Propulsion Laboratory (JPL)ephemerides [17]. There are 100 integration steps for trajectory propagation using the fourth-order fixed-step Runge–Kutta method. The 100 step integration leads to sufficient solution accuracy with the use of the orbital averaging method. With the direct optimization method, the obtained minimized transfer time is 66.8 days, and the propellant mass is 34.89 kg. The solutions solved via other methods give the transfer time of 66.6 [15,18], 67.0 [15],

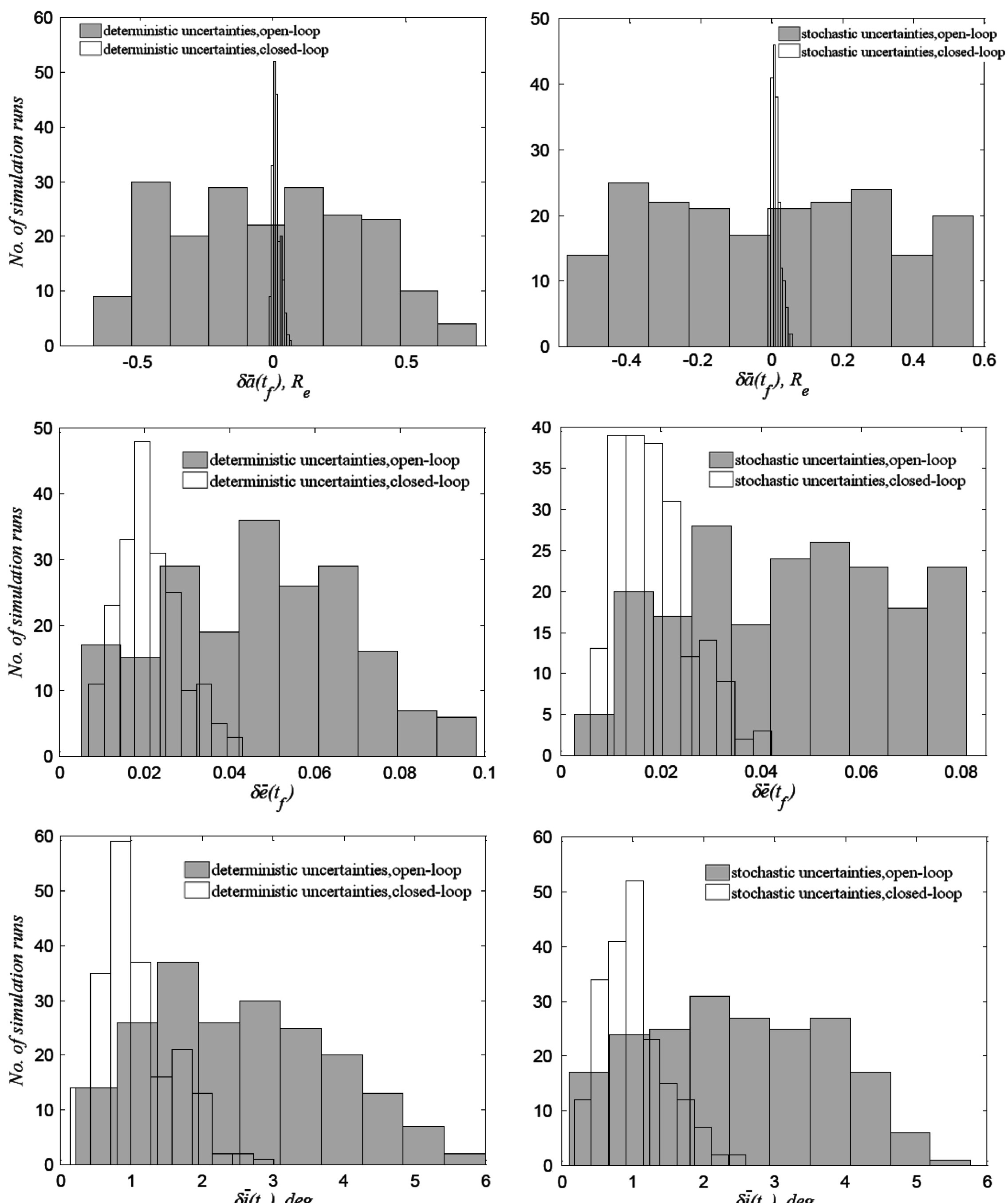

Fig. 1 Histograms of the terminal state errors $\delta\bar{a}(t_f)$, $\delta\bar{e}(t_f)$, and $\delta\bar{i}(t_f)$ with the Monte Carlo simulations.

and 70.2 days [16]. The optimal states $\bar{x}^*(t)$ and the controller parameter vector $\bar{\lambda}^*(t)$ are used to obtain the time-varying linear state-space model for guidance design, as well as stored onboard for trajectory tracking.

In the presence of the initial orbital deviations, unknown thrust direction misalignment and magnitude bias, unmodeled perturbations, and navigation noise, the guidance scheme should be able to guide the spacecraft to track the nominal trajectory. In the preliminary simulations, the semi-analytic trajectory propagation [9,10] is employed to verify the performance of the linear feedback guidance, which means that the numerical simulations are performed in the mean orbital element space. The $J_2 - J_5$ harmonics and lunar and sun perturbations are included. There are 100 AREs solved offline for obtaining the time-varying feedback gain $\boldsymbol{K}(t)$. To compute $\boldsymbol{K}(t)$, the weighting matrices $\boldsymbol{Q}$ and $\boldsymbol{R}$ are simply set to constant values as $\boldsymbol{Q} = \mathrm{diag}(2 \times 10^4, 10^5, 10^5, 10^6, 10^6)$ and $\boldsymbol{R} = \mathrm{diag}(10^2, 10^2, 10^2, 10^3, 10^3)$, where diag(.) means a matrix with the diagonal elements in the brackets. The values of $\boldsymbol{Q}$ and $\boldsymbol{R}$, chosen by trial and error, result in 100 closed-loop time-invariant linear control systems, each of which is valid over a 0.668 day subinterval. As a result, the nominal trajectory state (100 nodes for $\bar{x}(t)$ with a 5×1dimension each), the controller parameters (100 nodes for $\bar{\lambda}(t)$ with a 5×1 dimension each), as well as the feedback gain (100 nodes for $\boldsymbol{K}(t)$ with a 5×5 dimension each) are stored onboard for guidance. The navigation system is in charge of providing the orbital deviation $\delta\bar{x}(t)$.

Considering the presence of a wide range of errors in the initial orbital elements $\delta\bar{a}(t_0)$, $\delta\bar{e}(t_0)$, $\delta\bar{i}(t_0)$, $\delta\bar{\Omega}(t_0)$, and $\delta\bar{\omega}(t_0)$, and the uncertainties in thrust (unknown thrust direction misalignment and magnitude bias), it is necessary to run a large number of simulations to verify the performance of the guidance scheme using the Monte Carlo method. The uncertainties in thrust can be divided into two types: deterministic and stochastic. The deterministic uncertainties mean that the actual thrust output has unknown fixed deviation from control commands. The stochastic uncertainties in thrust come from the fact that the actual thrust output varies randomly in a range, not exactly matching control commands. For example, the stochastic uncertainties in thrust of the ion thruster equipped for the Deep Space 1 spacecraft were identified by low-thrust calibration [19]. For the preliminary simulation, the noise in the navigation system is generally considered a source that causes the stochastic uncertainties in thrust so that it is not separately modeled. Therefore, the orbital deviation $\delta\bar{x}(t)$ is simply deemed accurate for simulation.

First of all, deterministic uncertainties are included only for simulation. The terminal state errors $\delta\bar{a}(t_f)$, $\delta\bar{e}(t_f)$, and $\delta\bar{i}(t_f)$ are recorded by 200 simulation runs with both the open-loop and closed-loop controls. For each run, the errors in the initial orbital elements, unknown misalignment in thrust direction angles (δ and ϕ), and unknown bias in thrust magnitude are randomly selected according to the uniform distributions (with the uncertainty intervals listed in Table 1). Next, it is assumed that the stochastic uncertainties are included, but the deterministic uncertainties are not for each simulation run. The stochastic uncertainties in thrust (unknown misalignment and bias in Table 1) also follow uniform distributions with the uncertainty intervals listed in Table 1. Another 200 simulation runs (with both the open-loop and closed-loop controls) are performed to record the terminal state errors. The errors in the initial orbital elements are randomly selected (see Table 1) for each run. For all the simulation runs, the uncertainties in thrust direction angles or thrust magnitude (either deterministic or stochastic) are augmented to the computed values by the guidance algorithm to form the actual control at each numerical integration step. It is worth mentioning that the transfer time is set to the optimal value for every simulation run.

The histograms of the terminal state errors $\delta\bar{a}(t_f)$, $\delta\bar{e}(t_f)$, and $\delta\bar{i}(t_f)$ for all the simulation runs (200 runs for each case) are shown in Fig. 1. The simulation results show that the initial orbital errors and uncertainties in thrust may cause significant orbital deviations at the terminal time for the cases with the open-loop control only (most significant in the semimajor axis). The feedback guidance is useful to drive the spacecraft to return to its nominal trajectory. The differences in propellant consumption for all the runs lie in 1% of the nominal value, which is caused by slightly different shadowing conditions. The terminal state errors $\delta\bar{a}(t_f)$, $\delta\bar{e}(t_f)$, and $\delta\bar{i}(t_f)$ for the simulation runs with the closed-loop feedback guidance are on the orders of less than $0.05R_e$, 0.04, and 3 deg, respectively. For the final orbital insertions or rendezvous, such state errors can be eliminated by terminal guidance maneuvers.

Conclusions

A linear feedback guidance scheme for low-thrust many-revolution Earth-orbit transfers has been developed, and the preliminary numerical simulations have been carried out. The parameterized control law is employed in both optimization and guidance. This design concept differs from other approaches by establishing a standard form of a time-varying linear control system tackled by linear control theory. The feedback guidance accommodates system uncertainties and the predictive control depends on accurate system parameters. In addition, there is no need for computing appropriate control-related parameters using onboard iterative algorithms. The proposed guidance scheme implicitly possesses near-optimal performance because the optimal trajectory and control can be tracked via space crafts. Furthermore, with the use of orbital averaging, storing the nominal trajectory and control as well as the feedback gains onboard does not require memory hardware with large storage capacity. The approach for selecting feedback gains to achieve both optimality and robustness of the guidance scheme, which is a trial-and-error method in this note, will be studied in more detail in the future.

Acknowledgments

This work is supported by the National Natural Science Foundation of China (grant no. 10603005). The author would like to thank the Associate Editor and reviewers for their valuable comments and suggestions.

References

[1] Kluever, C. A., "Low-Thrust Orbit Transfer Guidance Using an Inverse Dynamics Approach," *Journal of Guidance, Control, and Dynamics*, Vol. 18, No. 1, 1995, pp. 187–189. doi:10.2514/3.56676

[2] Kluever, C. A., and Shaughnessy, D. J., "Trajectory-Tracking Guidance Law for Low-Thrust Earth-Orbit Transfers," *Journal of Guidance, Control, and Dynamics*, Vol. 23, No. 4, 2000, pp. 754–756. doi:10.2514/2.4597

[3] Ilgen, M. R., "Low Thrust OTV Guidance Using Lyapunov Optimal Feedback Control Techniques," AAS/AIAA Astrodynamics Specialist Conference, American Astronautical Society Paper 93-680, Aug. 1993.

[4] Chang, D. E., Chichka, D. F., and Marsden, J. E., "Lyapunov-Based Transfer Between Elliptic Keplerian Orbits," *Discrete and Continuous Dynamical Systems: Series B*, Vol. 2, No. 1, 2002, pp. 57–67.

[5] Petropoulos, A. E., "Low-Thrust Orbit Transfers Using Candidate Lyapunov Functions with a Mechanism for Coasting," AIAA/AAS Astrodynamics Specialist Conference, AIAA Paper 2004-5089, Aug. 2004.

[6] Gurfill, P., "Nonlinear Feedback Control of Low-Thrust Orbital Transfer in a Central Gravitational Field," *Acta Astronautica*, Vol. 60, No. 8–9, 2007, pp. 631–648. doi:10.1016/j.actaastro.2006.10.001

[7] Walker, M. J. H., Ireland, B., and Owens, J., "A Set of Modified Equinoctial Orbit Elements," *Celestial Mechanics and Dynamical Astronomy*, Vol. 36, No. 4, 1985, pp. 409–419.

[8] Gao, Y., and Kluever, C. A., "Low-Thrust Interplanetary Orbit Transfers Using Hybrid Trajectory Optimization Method with Multiple Shooting," AIAA/AAS Astrodynamics Specialist Conference, AIAA Paper 2004-5088, Aug. 2004.

[9] Cefola, P. J., Long, A. C., and Holloway, G., Jr., "The Long-Term Prediction of Artificial Satellite Orbits," AIAA 12th Aerospace Sciences Meeting, AIAA Paper 1974-170, 1974.

[10] Danielson, D. A., Sagovac, C. P., Neta, B., and Early, L. W., "Semi-Analytic Satellite Theory," U.S. Naval Postgraduate School TR MA-95-002, Monterey, CA, 1995.

[11] Bryson, A. E., and Ho, Y. C., *Applied Optimal Control*, Wiley, New

York, 1975, pp. 65–69.
[12] Pouliot, M. R., "CONOPT2: A Rapidly Convergent Constrained Trajectory Optimization Program for TRAJEX," General Dynamics SP-82-008, San Diego, CA, 1982.
[13] Betts, J. T., "Survey of Numerical Methods for Trajectory Optimization," *Journal of Guidance, Control, and Dynamics*, Vol. 21, No. 2, 1998, pp. 193–207.
doi:10.2514/2.4231
[14] Lewis, F. L., *Optimal Control*, Wiley, New York, 1986, pp. 189–209, 221–228.
[15] Kluever, C. A., and Oleson, S. R., "Direct Approach for Computing Near-Optimal Low-Thrust Earth-Orbit Transfers," *Journal of Spacecraft and Rockets*, Vol. 35, No. 4, 1998, pp. 509–515.
doi:10.2514/2.3360
[16] Gao, Y., "Near-Optimal Very Low-Thrust Earth-Orbit Transfers and Guidance Schemes," *Journal of Guidance, Control, and Dynamics*, Vol. 30, No. 2, 2007, pp. 529–539.
doi:10.2514/1.24836
[17] Standish, E. M., "The JPL Planetary and Lunar Ephemerides DE402/LE402," *Bulletin of the American Astronomical Society*, Vol. 27, 1995, p. 1203.
[18] Sackett, L. L., Malchow, H. L., and Edelbaum, T. N., "Solar Electric Geocentric Transfer with Attitude Constraints: Analysis," NASA CR-134927, Aug. 1975.
[19] Wolff, P. J., Pinto, F., Williams, R. M., and Vaughan, R. M., "Navigation Considerations for Low-Thrust Planetary Missions," AAS/AIAA Space Flight Mechanics Meeting, American Astronautical Society Paper 98-201, 1998.

B. Marchand
Associate Editor